Aspects of Charge Distribution Measurement for [superscript 252]Cf(sf)

Aspects of charge distribution measurement for ^{252}Cf(sf)

Taofeng Wang,[1,2,3,4,*] Guangwu Li,[5] Liping Zhu,[5] Or Hen,[2] Gaolong Zhang,[1,3,4] Qinghua Meng,[5] Liming Wang,[5] Hongyin Han,[5] and Haihong Xia[5]

[1]*School of Physics and Nuclear Energy Engineering, Beihang University, Beijing 100191, China*
[2]*Department of Physics, Massachusetts Institute of Technology, Cambridge, Massachusetts 02139, USA*
[3]*International Research Center for Nuclei and Particles in the Cosmos, Beihang University, Beijing 100191, China*
[4]*Beijing Key Laboratory of Advanced Nuclear Materials and Physics, Beihang University, Beijing 100191, China*
[5]*China Institute of Atomic Energy, P.O. Box 275-46, Beijing 102413, China*

(Received 10 July 2017; published 19 September 2017)

Measurements of charge distributions of fragments in the spontaneous fission of ^{252}Cf have been performed using a unique detector setup consisting of a typical grid-ionization chamber coupled with a ΔE-E charged particle telescope. We find that the fragment mass dependency of the kinetic-energy-averaged width of the charge distribution shows a systematically decreasing trend with obvious fluctuations. The variation of the widths of the charge distribution with kinetic energy shows a pan-like shape. This is due to the large number of neutrons emitted at the high excitation energies and cold fragmentation at the low excitation energies. Deviation of the kinetic-energy-averaged most probable charge Z_p from the unchanged charge distribution (UCD), ΔZ, as a function of the mass number of primary fragments, A^*, changes from negative for mass asymmetric fission to positive near the symmetric fissions. Concerning the kinetic energy dependence of Z_p given primary mass number A^*, obvious increasing tendencies of Z_p with increasing kinetic energy are observed.

DOI: 10.1103/PhysRevC.96.034611

I. INTRODUCTION

The nuclear fission reaction is a complex process involving nuclear dynamics in which rearrangement of nuclear matter takes place during the descent from the saddle point to the scission. The investigations of the mass, nuclear charge, and kinetic energy distributions of fragments, as well as observations of correlations between these physical quantities, are of vast interest. Not only can they provide valuable information on the probability of coupling collective modes to particle excitation degrees of freedom, but they can also contribute to exploration of the delicate interplay between the macroscopic aspects of bulk nuclear matter and the quantum effects of a finite nuclear system. The mass and kinetic energy distribution of fragments have been studied for almost all known fission systems, including spontaneous fission and the low energy fission reactions induced by neutrons and other light particles. However, studies of the charge distribution of fragments, at various excitation energies and fragment mass numbers, are scarce due to the difficulty of assigning the nuclear charge and the mass numbers of fission fragments simultaneously.

In this work, isobaric charge distributions of fission fragments are represented in terms of the most probable charge Z_p and the standard deviation σ_Z, which provide useful information regarding the dynamics of the descent. The significant characteristics are the variance of Z_p and σ_Z dependence on excitation energy or kinetic energy of the fission fragments. Additional attention is given to the charge polarization (ΔZ), defined as the difference between the average most probable charge $Z_{p_{\rm ave}}$ and the charge expected on the basis of unchanged charge distribution (Z_{UCD}).

*tfwang@buaa.edu.cn

II. EXPERIMENTAL PROCEDURE

Radiochemical methods [1] as well as several physical approaches [2–9] have been adopted to extract the nuclear charge distribution of fragments in fission reactions. Mass spectrometry using fragment residual energy detection [3,10] or ΔE-E ionization [11] shows good nuclear charge resolution for studying the variation of the charge distribution with mass numbers and kinetic energy of fragments in a wide mass region [3]. A fragment with a certain mass number and an ionic charge state q at a given kinetic energy was selected by the LOHENGRIN spectrograph (Institut Laue-Langevin, Grenoble, France). The nuclear charge was determined by the residual energy of the fragment passing through an absorber [3], or by the energy deposition in a ΔE detector [11]. In contrast with this method, in the present work the detector system shown in Fig. 1 [12], consisting of a grid-ionization chamber (GIC) on the left side and a gas ΔE detector (a thin grid-ionization chamber) coupled with a supplementary surface-barrier detector (SBD) as E detector on the right side, which provide both ΔE and residual kinetic energy of the fragment, was used to investigate the nuclear charge distribution of fragments of spontaneous fission of ^{252}Cf.

Regarding the nuclear charge distribution, the approach employed in Ref. [6] by Knitter *et al.* explored the Z dependence of quantity $\overline{X}$, which is a measurement of the distance of the center of gravity of the electron-ion pair track from the origin of the trace, given by a general function of fragment kinetic energy E, mass A, and charge Z. The distributions of charge for light fragments with given mass values were extracted using multi-Gaussian function fitting. Concerning the present experiment, fragments with a certain mass number and kinetic energy were selected for nuclear charge determination via their energy deposition in ΔE and

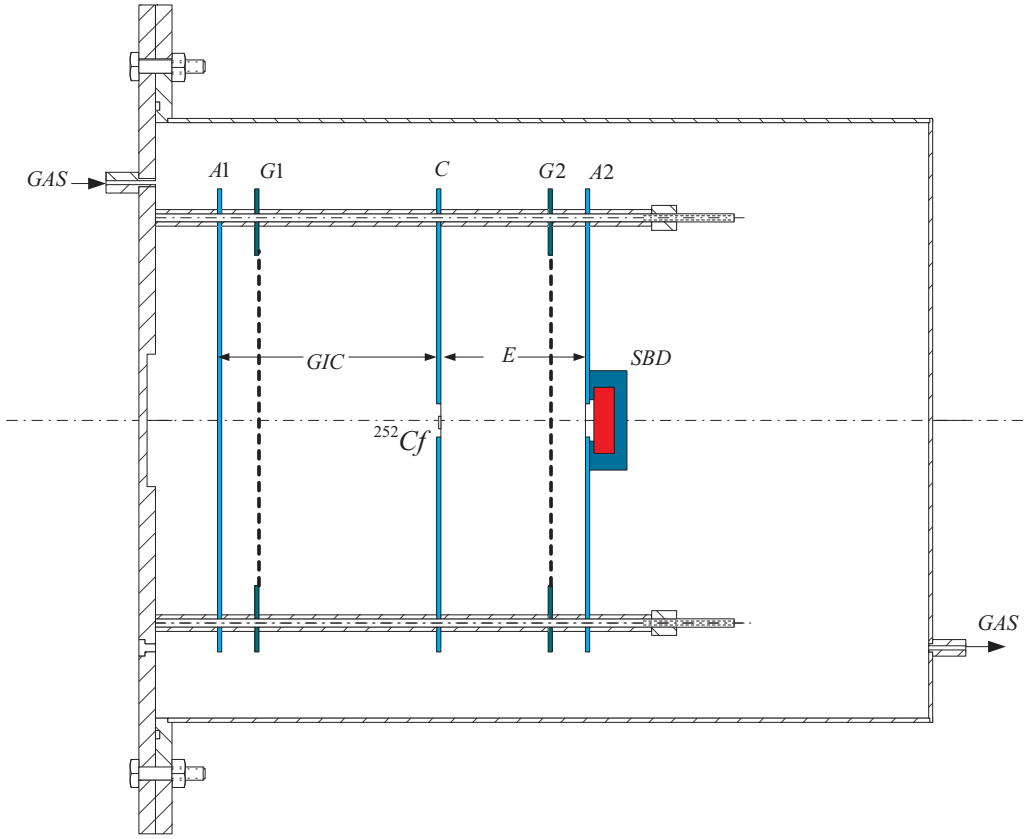

FIG. 1. Schematic view of the grid-ionization chamber coupled with a charged particle telescope detector system [12].

E detectors. Masses of the fission fragments are determined by the double energies method. The charge distributions of the light fragments for fixed mass number and kinetic energy were obtained using least-squares fits for the response functions of the ΔE detector with multi-Gaussian functions representing the different element charges. The results of the charge distributions for some typical fragments indicate that this detection setup has a charge distribution separation capability of $Z{:}\Delta Z > 40{:}1$. A detailed description of the experimental procedure is shown in a previous publication [12].

The fits for the ΔE spectrum using multi-Gaussian functions with the conditions (a) $A^* = 86$ u, $E^*_{kL} = 105$–108 MeV and (b) $A^* = 99$ u, $E^*_{kL} = 120$–123 MeV are shown in Fig. 2. The obvious structure in the distribution, the full width at half maximum (FWHM) of each Gaussian, is around 0.8, implying that the charge resolution of $Z{:}\Delta Z > 40{:}1$ has been obtained. In order to improve the statistics, we use 3 MeV kinetic energy bins in the data analysis. The average total fragment kinetic energy $\langle \mathrm{TKE} \rangle$ of the ^{252}Cf spontaneous fission reaction is 184.6 ± 1.3 MeV. For a light fragment with kinetic energy 125 MeV, the mass resolution of the present experimental setup is estimated to be $\sim$1.5 u from energy resolutions of GIC and SBD on the basis of the momentum and mass conservation. An iteration method of obtaining preneutron mass values through mean neutron multiplicities is employed in the data analysis procedure. The variation of the widths of the charge distributions with the fragment mass and the kinetic energy, the charge polarization as a function of the fragment mass, and the dependence of the most probable charge on kinetic energy and mass are discussed in the following session.

III. RESULTS AND DISCUSSION

A. Isobaric yield distribution

While the ΔE distributions for the selected light fragment mass and kinetic energy with an energy bin of 3.0 MeV were derived, we utilized a least squares fit on the ΔE spectrum with multi-Gaussian functions representing the nuclear charge distributions of the isobaric chain. The fractional independent yield (FIY) together with the charge distribution parameters—the most probable charge Z_p and the dispersion σ_Z dependent on kinetic energy—average most probable charge $Z_{p_{\mathrm{ave}}}$ and kinetic energy averaged dispersion $\sigma_{Z_{\mathrm{ave}}}$ of the charge distributions are obtained. Table I shows the FIY and charge distributions of light fragment $A^* = 101$ u under various kinetic energy conditions. ΔZ, $Z_{p_{\mathrm{ave}}}$ and $\sigma_{Z_{\mathrm{ave}}}$ are deduced to be -1.185 ± 0.012, 40.463 ± 0.012, and 0.6009 ± 0.0013. The uncertainties of the parameters (Z_p, σ_Z, $Z_{p_{\mathrm{ave}}}$, and $\sigma_{Z_{\mathrm{ave}}}$) result from the statistics errors in the fits with Gaussian functions. There are a number of mass chains where it has been possible to determine the independent yields of more than one isobar. Figure 3 shows the charge dispersion for fission products with $A^* = 101$ u and an average kinetic energy of 118.5 MeV under a Gaussian fit for the independent yields of ^{101}Y, ^{101}Zr, ^{101}Nb, ^{101}Mo, as well as ^{101}Tc. Deduced results of other mass chains exhibit a similar distribution; the width

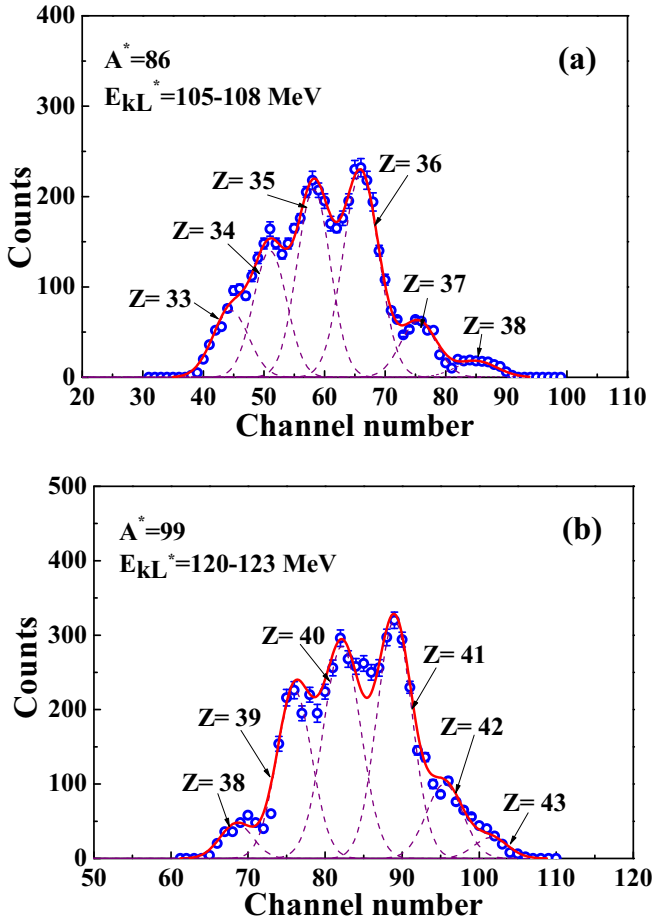

FIG. 2. The fitting for ΔE spectra using multi-Gaussian functions with the conditions (a) $A^* = 86$ u, $E^*_{kL} = 105$–108 MeV; (b) $A^* = 99$ u, $E^*_{kL} = 120$–123 MeV [12].

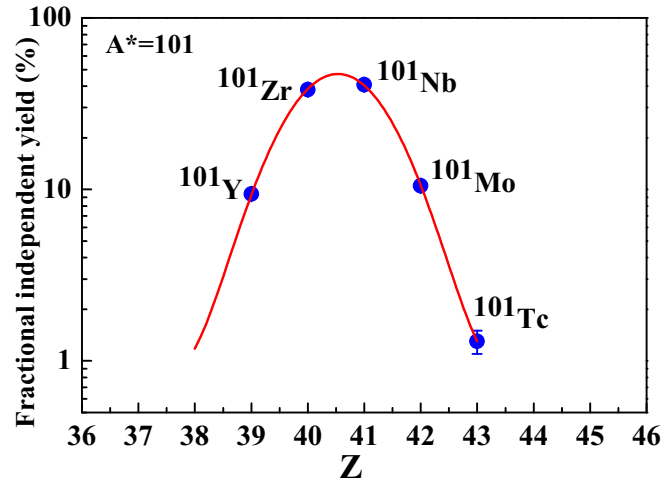

FIG. 3. Charge dispersion for products with $A^* = 101$ u and 118.5 MeV average kinetic energy.

of the distribution generally varies little with the variation of the isobaric mass number.

Figure 4 shows the averaged width $\sigma_{Z_{\rm ave}}$ of the charge distribution depending on the primary fission fragment mass A^*. The systematic trend of $\sigma_{Z_{\rm ave}}$ is decreasing when the primary fragment's mass number A^* increases. $d\sigma_{Z_{\rm ave}}/dA^* = -0.0117$ has been obtained from the linear fitting which is shown in Fig. 4. The largest deviation from the linear fitting occurs in the mass region ∼85, where nuclei have a near magic character ($N = 50$). It is experimentally known that the average neutron multiplicities are extremely low for fragments near the shell closures, namely, the excitation energy is rather low. On the other hand, the oscillating feature of $\sigma_{Z_{\rm ave}}$ as a function of A^* [13,14] indicates the presence of the odd-even effect. Two pronounced peaks at $A^* = 85$ and 122 u are likely caused by shell structure. The calculation results with GEF-2015-1-1 code [15] are also given in Fig. 4, in which a mostly flat trend is exhibited with fluctuations due to the known odd-even effect.

The rms width σ_Z of each charge-state distribution, dependent on the kinetic energy of light fragments with certain masses, are plotted in Fig. 5. The prominent feature is that σ_Z has a decreasing tendency in the case where kinetic energy E^*_{kL} is less than 110 MeV. Correspondingly, σ_Z shows

TABLE I. Fractional independent yields and charge distributions of light fragment $A^* = 101$ u for various kinetic energies.

E^*_{kL}/MeV	$Z = 37$	38	39	40	41	42	43	Z_p	σ_Z
84–87	3.9 ± 0.6	9.7 ± 1.0	28.7 ± 1.8	57.7 ± 2.9				39.40 ± 0.36	0.818 ± 0.040
87–90	1.6 ± 0.3	11.1 ± 0.8	29.1 ± 1.4	58.3 ± 2.2				39.44 ± 0.21	0.750 ± 0.019
90–93	2.3 ± 0.2	11.0 ± 0.2	20.3 ± 0.8	66.4 ± 1.6				39.51 ± 0.11	0.779 ± 0.013
93–96		3.3 ± 0.2	20.2 ± 0.6	76.5 ± 1.3				39.73 ± 0.07	0.512 ± 0.005
96–99		1.9 ± 0.1	11.6 ± 0.3	44.3 ± 0.7	42.2 ± 0.7			40.27 ± 0.05	0.737 ± 0.006
99–102		0.57 ± 0.05	8.8 ± 0.2	41.6 ± 0.6	49.0 ± 0.6			40.39 ± 0.04	0.669 ± 0.004
102–105		2.2 ± 0.1	13.8 ± 0.2	51.4 ± 0.5	32.6 ± 0.4			40.14 ± 0.03	0.729 ± 0.004
105–108			4.8 ± 0.1	42.3 ± 0.4	52.8 ± 0.5			40.48 ± 0.03	0.589 ± 0.003
108–111			3.3 ± 0.1	32.1 ± 0.4	64.6 ± 0.6			40.61 ± 0.03	0.551 ± 0.004
111–114				17.6 ± 0.3	74.4 ± 0.8	7.9 ± 0.2		40.90 ± 0.03	0.496 ± 0.003
114–117			2.0 ± 0.1	45.9 ± 0.8	51.0 ± 0.8	1.1 ± 0.1		40.51 ± 0.04	0.559 ± 0.004
117–120			9.4 ± 0.5	38.2 ± 1.1	40.7 ± 1.1	10.5 ± 0.5	1.3 ± 0.2	40.56 ± 0.04	0.849 ± 0.008
120–123			28.7 ± 1.6	41.9 ± 2.0	24.5 ± 1.5	3.3 ± 0.5	1.6 ± 0.3	40.07 ± 0.14	0.897 ± 0.021
123–126			17.3 ± 2.2	36.9 ± 3.5	24.0 ± 2.7	13.9 ± 2.0	7.9 ± 1.4	40.58 ± 0.41	1.160 ± 0.100

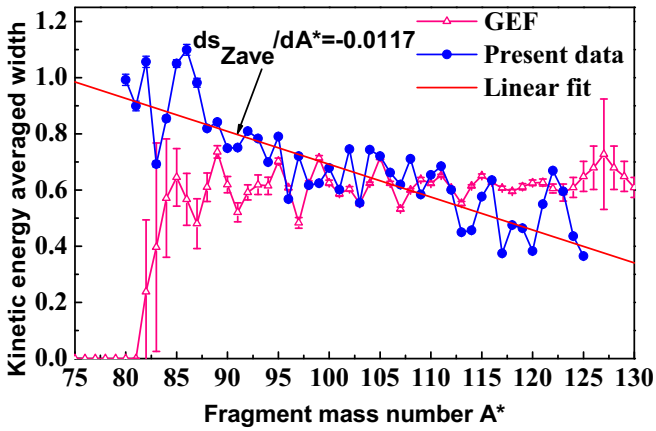

FIG. 4. The fragment mass dependency of kinetic energy averaged widths $\sigma_{Z_{ave}}$ of the charge distributions; the solid points indicate the present experimental data, the triangles represent the calculation results from GEF code [15], and the solid line is the linear function fitting.

an increasing trend for E^*_{kL} greater than 110 MeV. In the other words, the parameters of charge distributions vary not only with the fragment mass, but also with the excited energy of fission compound nucleus. Comparing the mass and charge distributions for the same fission reactions, one notices that asymmetric distributions are observed for both the mass and the charge yields with the peak/valley ratios for asymmetric/symmetric splits of the parent nucleus. It suggests that fragment mass and fragment charge are rather intimately linked [16]. From the broadening of the mass distributions at larger excitation energies of the compound nucleus, one should also expect the global charge distributions of fragments to become wider at higher temperatures, provided that the correlation between fragment mass and charge addressed above remains valid. However, as seen from Fig. 5, the trends for the widths σ_Z of charge distributions are not a linear function of the kinetic energies (or excitation energies). Minimum values of σ_Z exist at around 110 MeV of E^*_{kL}, which is the average kinetic energy of light fragments of ^{252}Cf. In other words, a complex correlation was observed for the width of charge distribution and the excitation energy of fragments.

The difference in the σ_Z variation with kinetic energy may be comprehended from the fact that lower kinetic energies correspond to higher excitation energies, hence the number of evaporated neutrons will be larger. For large neutron number ν their variance $\sigma^2(\nu)$ is also large, and therefore a given primary mass A^* together with its intrinsic charge distribution will be spread over a wider range of fission product mass A. As a result, the smaller the kinetic energy of the fission products, the more the charge variance measured should rise compared to the variance of the primary fragments [16]. It is interesting to analyze the evolution of fragment charge distributions up to the highest feasible kinetic energies, namely, in cold fission for which fragments have such low excitation energy that no neutrons are emitted. The fragments are probably produced with ground-state deformation in their ground states. According to the quantum-mechanical zero-point vibration, the fragment elongations in fission have a large variation range with an elongating uncertainty of the order of 1–2 fm [6]. For a typical fragment split yielding ^{109}Tc and ^{143}Cs in the spontaneous fission of ^{252}Cf, the deformation energy for Tc

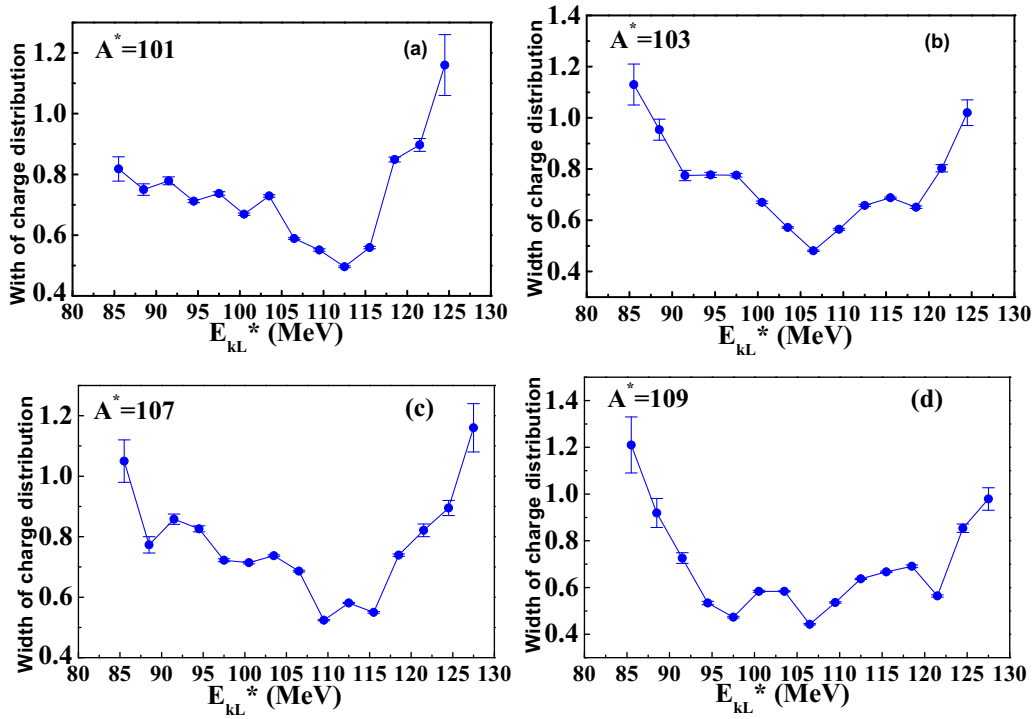

FIG. 5. The widths σ_Z of charge distributions depend on the kinetic energy of the light fragments E^*_{kL}: (a), (b), (c), and (d) correspond to the primary fragment masses 101, 103, 107, and 109 u, respectively.

is estimated to be about 6.5 MeV/fm. Figure 5 shows the σ_Z variation with kinetic energy on $A^* = 101$, 103, 107, and 109 u, which probably represents the typical fragment splits holding large elongation uncertainty; consequently large σ_Z are produced.

During the charge equilibrium at a fixed mass value, the charge equilibrium mode N/Z is generally represented by a harmonic oscillator having a phonon energy $\hbar\omega$ of a few MeV for a nucleus at scission, which has the characteristic of giant dipole resonance [17,18]. This oscillator is coupled to the intrinsic degrees of freedom. Under these condition the standard deviation of charge $\langle\sigma_Z^2\rangle$ depends on the nuclear temperature T and the inertial parameter of N/Z mode M:

$$\langle\sigma_Z^2\rangle = \frac{1}{M\omega^2}\left(\frac{1}{2}\hbar\omega + \frac{\hbar\omega}{e^{\hbar\omega/T}-1}\right). \quad (1)$$

Obviously, from Fig. 5 a decrease can be observed with increasing (decreasing) kinetic (excitation) energy for $E^*_{kL} <$ 110 MeV, which can be understood with the above equation, since the nuclear temperature T is related to excitation energy E_x by $E_x = aT^2$ with $a = \frac{1}{8}A$ from [3]. Djebara *et al.* shows a flat behavior of $\langle\sigma_z^2\rangle$ for different fissioning systems [10], which is explained by the zero-point oscillation of a collective-isovector giant dipole resonance of the compound nuclear system at the scission point. The dependence of $\langle\sigma_z^2\rangle$ on kinetic energy should have a dynamical origin through the change of neck radius c with time. Nifenecker found that the asymptotic ($t \to \infty$) value of the charge variance $\langle\sigma_z^2\rangle$ increases strongly with the necking velocity (dc/dt), i.e., the speed at which the neck pinches off [19,20], showing that $\langle\sigma_z^2\rangle$ has a linear correlation with dc/dt, which accounts for the increasing trend at the highest kinetic energy ($E^*_{kL} >$ 110 MeV) in Fig. 5. Brissot and Bocquet [17] clearly showed that the collapse of the neck is five times faster for ^{250}Cf* than ^{230}Th*. The increase of σ_z indicates that the velocity of pinching of the neck quickly increases with the highest kinetic energies for cold fission. $\langle\sigma_Z^2\rangle$ decrease with parameter M related to N/Z according to Eq. (1), which can explain the $\sigma_{Z_{\rm ave}}(A^*)$ variations with fragment mass number A^* in Fig. 4. The calculation of $\sigma_{Z_{\rm ave}}(A^*)$ with GEF shows a flat trend having a little fluctuation.

B. Charge polarization

An important approach regarding the nuclear charge distribution in fission is to investigate the behavior of the average most probable charge $Z_{p_{\rm ave}}$ with respect to its deviation ΔZ from the unchanged charge distribution (UCD) as a function of the mass number of primary fragments A^* [21]:

$$\Delta Z = (Z_{p_{\rm ave}} - Z_{UCD})_H = (Z_{UCD} - Z_{p_{\rm ave}})_L, \quad (2)$$

$$Z_{UCD} = (Z_F/A_F) \times [A + \overline{\nu}(A^*,\mathrm{TKE})], \quad (3)$$

where H and L designate the heavy and light fragments, respectively, and TKE is the total kinetic energy of fragments. Z_F and A_F are charge and mass of the fissioning system. $\overline{\nu}(A^*,\mathrm{TKE})$ is the number of neutrons emitted by the corresponding fission fragment, which is taken from Ref. [22].

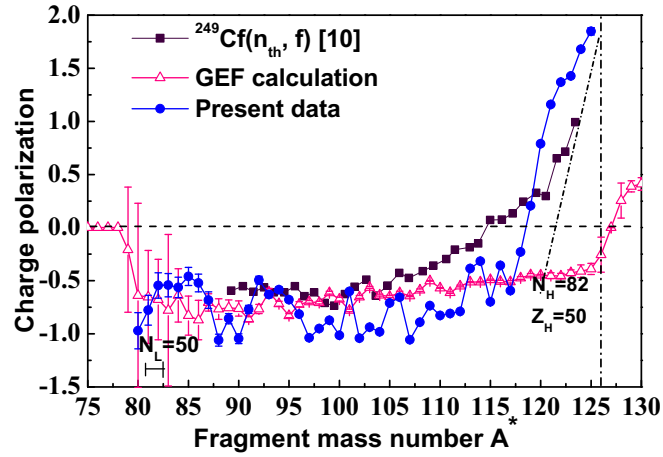

FIG. 6. Charge polarization ΔZ as a function of the mass number of primary fission fragments A^*. The solid points indicate the present experimental data, the triangles represent the calculation results from GEF code [15]. The dotted line indicates the neutron number $N_H = 82$ and proton number $Z_H = 50$ for heavy fragments. The dash-dotted line indicates the symmetry fission.

The charge polarization as a function of primary fragment mass A^* is shown in Fig. 6, which is similar to the results of Djebara [10]. Djebara's work considered the thermal neutron-induced fission of ^{249}Cf. This system is different from spontaneous fission ^{252}Cf studied in the present work; in particular the excitation energy in thermal neutron-induced fission of ^{249}Cf is higher (the neutron separation energy of ^{250}Cf is 6.6 MeV). The main characteristics of ΔZ emerging from the figure are that for asymmetric fission ($A^*_L < 120$) ΔZ is a negative value which exhibits marked fluctuations due to odd-even effects, while upon approaching mass symmetry ($A^*_L \geqslant 120$) ΔZ turns positive and does not fluctuate. The spectacular change of sign for ΔZ was not anticipated by theory. For the asymmetric mass split region the fragments are polarized in charge, with more than half a proton being transferred from the heavy to the light fragment. The heavy fragment with the closed proton shell $Z = 50$ may play an essential role, causing the charge deviation ΔZ to reverse sign. The size of odd-even fluctuations in $\Delta Z(A^*)$ decreases with increasing fissility Z_F^2/A_F and increasing excitation energy of the fissioning nucleus (Z_F, A_F) [16]. The calculation for $\Delta Z(A^*)$ with GEF code is also shown in Fig. 6; the average value of present data is close to that from the GEF calculation except for the region near the magic number ($N = 50$).

C. The dependence of Z_p on E^*_{kL}

The dependence of the most probable charge Z_p on fragment kinetic energy E^*_{kL} is shown in Fig. 7, where the primary mass numbers of light fragments are given. The obvious increasing tendencies for Z_p with the kinetic energies, which are measured for the first time, emerge from the figures. It can be seen that Z_p of light fragment mass chains vary with energy in similar ways. It is likely that the nuclear charge distribution between the primary fragments is controlled by a process that is unaltered by additional excitation in the

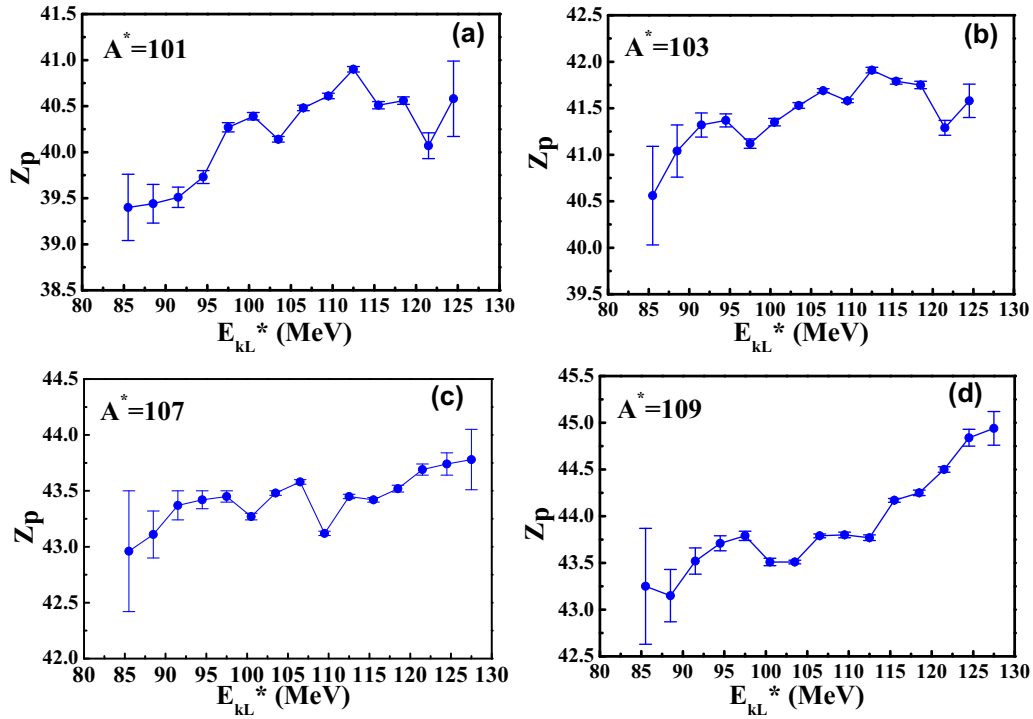

FIG. 7. Kinetic fragment energies dependence of the most probable charge Z_p for ^{252}Cf: (a), (b), (c), and (d) corresponding to the primary fragment masses 101, 103, 107, and 109 u, respectively.

compound nucleus; hence, the resultant change in Z_p with kinetic energy (or excitation energy) is due only to increased neutron emission at higher excitations [23]. This similar variation in Z_p with energy adds support to the assumption of an identical charge dispersion in the mass chains. The energy ($E^*_{kL} > 110$ MeV) is well above average and, in fact, one is approaching cold fission, where all of the available reaction energy $Q(A,Z)$ is converted into fragment kinetic energy. Upon coming close to cold fission, it is found that in most cases the charge number $Z(A)$ maximizing the yield $Y(Z|A)$ for given mass number A coincides with the charge maximizing reaction energy $Q(Z|A)$ [16]. The variation of Z_p of the charge distribution in a given isobaric chain is related only to prompt neutron emission, which makes the fragment nucleus shift closer to the valley of β stability. On the other hand, it is connected to a decrease of the charge polarization in primary fission fragments, which causes a reduction of charge density of light fragments and an increase of charge density of heavy fragments [24,25]. With the increasing excitation energy of the compound nucleus, the primary heavy products therefore are near the line of β stability and primary light products are away from it. This effect decreases the most probable charge of light fission fragments and increases it for heavy fragments.

The average charge of isobaric chains vs the mass number of light fission products is shown in Fig. 8. The results of calculations from Waldo's $Z_{p_{\rm ave}}(A)$ formula [26] are also exhibited in the figure:

$$Z_{p_{\rm ave}}(A) = 0.4153A - 1.19 + 0.167(236 - 92A_F/C_F), \quad A < 116, \tag{4}$$

$$Z_{p_{\rm ave}}(A) = 0.4153A - 3.43 + 0.243(236 - 92A_F/C_F), \quad A > 116, \tag{5}$$

where C_F is the charge number of fissioning nuclei. It can be seen from this figure that the present data are in a perfect agreement with the results calculated with Waldo's formula [26].

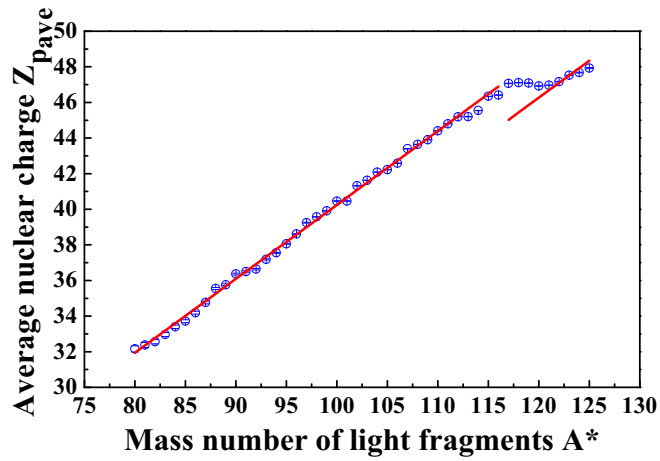

FIG. 8. The average most probable charge $Z_{p_{\rm ave}}$ as a function of mass number of light fragments for ^{252}Cf. The solid curve is the results of calculations using Waldo's formula.

IV. CONCLUSION

The measurement of charge distributions of fragments in spontaneous fission ^{252}Cf was performed by using a unique style of detector setup consisting of a typical grid ionization chamber and a ΔE-E particle telescope in which a thin grid ionization chamber served as the ΔE section and the E section was a surface barrier detector. The typical physical quantities of fragments, such as mass number and kinetic energies, as well as the deposition in the gas ΔE detector and E detector, were derived from the coincident measurement data. The charge distributions of the light fragments for fixed mass number and kinetic energy were obtained by least-squares fits for the response functions of the ΔE detector with multi-Gaussian functions representing the different element charges. The results of the charge distributions for some typical fragments are shown in this article; they indicate that this detection setup has the charge distribution capability $Z{:}\Delta Z \geqslant 40{:}1$.

A result of the study is that the fragment mass dependency of the average width of the charge distribution shows a systematic decreasing trend with an obvious odd-even effect. For the variation of widths of charge distribution with light fragment products' kinetic energies, approximately V-shaped curves were observed due to the large number of neutrons emitted at low kinetic energies (or high excitation energies) and the approaching cold fission for high kinetic energies ($E^*_{kL} > 110$ MeV). Concerning the behavior of the average most probable charge $Z_{p_{\rm ave}}$ with respect to its deviation ΔZ from the unchanged charge distribution (UCD) as a function of the mass number of primary fragments A^*, for asymmetric fission products ($A^*_L < 120$) ΔZ is a negative value which exhibits marked fluctuations due to odd-even effects, while upon approaching mass symmetry ($A^*_L \geqslant 120$) ΔZ turns positive and does not fluctuate. It is likely that for the asymmetric mass split region the fragments are polarized in charge, with more than half a proton being transferred from the heavy to the light fragment. It is possible that heavy magic fragments with the closed proton shell $Z = 50$ may play a role, causing the charge deviation ΔZ to reverse sign. Concerning the energy dependence of the most probable charge Z_p for given primary mass number A^*, the obvious increasing tendencies of Z_p with the kinetic energies E^*_{kL} are observed for the first time. This phenomenon is due only to increased neutron emission at higher excitations. The correlation between the average nuclear charge and the primary mass number is given as a linear function, which is in perfect agreement with the calculated results using Waldo's formula.

ACKNOWLEDGMENTS

This work has been supported by the National Natural Science Foundation of China (Grants No. 10175091, No. 11305007, and No. 11235002).

[1] A. Ramaswaswami, G. K. Gubbi, R. J. Singh, and S. Prakash, J. Radiol. Nucl. Chem. **125**, 85 (1988).
[2] H. W. Schmitt, W. E. Kiker, and C. W. Williams, Phys. Rev. **137**, B837 (1965).
[3] W. Lang, H.-G. Clerc, and H. Wohlfarth, Nucl. Phys. A **345**, 34 (1980).
[4] G. Mariolopoulos, J. P. Bocquet, and R. Brissot, Nucl. Instrum. Methods **180**, 141 (1981).
[5] M. Djebara, M. Asghar, and J. P. Bocquet, Nucl. Phys. A **425**, 120 (1984).
[6] H.-H. Knitter, F.-J.Hambsch, and C. Budtz-Jørgensen, Nucl. Phys. A **536**, 221 (1992).
[7] F.-J.Hambsch, H.-H. Knitter, and C. Budtz-Jørgensen, Nucl. Phys. A **554**, 209 (1993).
[8] J. B. Wilhelmy, E. Cheifetz, and R. C. Jared, Phys. Rev. C **5**, 2041 (1972).
[9] G. M. Ter-Akopian, J. H. Hamilton, Y. T. Oganessian *et al.*, Phys. Rev. Lett. **77**, 32 (1996).
[10] M. Djebara, M. Asghar, and J. P. Bocquet, Nucl. Phys. A **496**, 346 (1989).
[11] J. L. Sida, P. Armbruster, and M. Bernas, Nucl. Phys. A **502**, 233c (1989).
[12] T. Wang, H. Han, and Q. Meng, Nucl. Instrum. Methods Phys. Res., Sect. A **697**, 7 (2013).
[13] A. Notea, Phys. Rev. **182**, 1331 (1969).
[14] B. Wilkins, E. Steinberg, and R. Chasman, Phys. Rev. C **14**, 1832 (1976).
[15] K. Schmidt and B. Jurado, Eur. Phys. J. A **51**, 176 (2015).
[16] C. Wagemans, in *The Nuclear Fission Process* (CRC, Boca Raton, FL, 1991), p. 394.
[17] J. P. Bocquet and R. Brissot, Nucl. Phys. A **502**, 213 (1989).
[18] M. Berlanger, A. Gobbi, and F. Hannape, Z. Phys. A **291**, 133 (1979).
[19] H. Nifenecker, J. Phys. Lett. **41**, 47 (1980).
[20] H. Naik, S. P. Dange, and R. J. Singh, Nucl. Phys. A **612**, 143 (1997).
[21] H. Naik, R. J. Singh, and R. H. Iyer, Eur. Phys. J. A **16**, 495 (2003).
[22] C. Budtz-Jørgensen, Nucl. Phys. A **490**, 307 (1988).
[23] J. A. Mchugh and M. C. Michel, Phys. Rev. **172**, 1160 (1968).
[24] T. Wang, G. Li, L. Zhu *et al.*, Phys. Rev. C **93**, 014606 (2016).
[25] V. A. Roshchenko, V. M. Piksaikin, S. G. Isaev, and A. A. Goverdovski, Phys. Rev. C **74**, 014607 (2006).
[26] R. W. Waldo, R. A. Karam, and R. A. Meyer, Phys. Rev. C **23**, 1113 (1981).